

A Si-Cl geothermobarometer for the reaction zone of high-temperature, basaltic-hosted mid-ocean ridge hydrothermal systems

Fabrice Fontaine, William Wilcock, Dionysis Foustoukos, David Butterfield

► **To cite this version:**

Fabrice Fontaine, William Wilcock, Dionysis Foustoukos, David Butterfield. A Si-Cl geothermobarometer for the reaction zone of high-temperature, basaltic-hosted mid-ocean ridge hydrothermal systems. *Geochemistry, Geophysics, Geosystems*, AGU and the Geochemical Society, 2009, 10 (5), 10.1029/2009GC002407 . insu-01731458

HAL Id: insu-01731458

<https://hal-insu.archives-ouvertes.fr/insu-01731458>

Submitted on 14 Mar 2018

HAL is a multi-disciplinary open access archive for the deposit and dissemination of scientific research documents, whether they are published or not. The documents may come from teaching and research institutions in France or abroad, or from public or private research centers.

L'archive ouverte pluridisciplinaire **HAL**, est destinée au dépôt et à la diffusion de documents scientifiques de niveau recherche, publiés ou non, émanant des établissements d'enseignement et de recherche français ou étrangers, des laboratoires publics ou privés.



A Si-Cl geothermobarometer for the reaction zone of high-temperature, basaltic-hosted mid-ocean ridge hydrothermal systems

Fabrice J. Fontaine

School of Oceanography, University of Washington, Box 357940, Seattle, Washington 98195-7940, USA

Now at Institut de Physique du Globe de Paris, UMR7154, Université Paris 7-Denis Diderot, CNRS, 4 place Jussieu, F-75252 Paris CEDEX 05, France (fontaine@ipgp.jussieu.fr)

William S. D. Wilcock

School of Oceanography, University of Washington, Box 357940, Seattle, Washington 98195-7940, USA

Dionysis E. Foustoukos

Geophysical Laboratory, Carnegie Institution of Washington, 5251 Broad Branch Road NW, Washington, D. C. 20015, USA

David A. Butterfield

Joint Institute for the Study of the Atmosphere and Oceans, University of Washington, 7600 Sand Point Way NE, Seattle, Washington 98115, USA

[1] The chemical composition of mid-ocean ridge hydrothermal vent fluids is thought to reflect conditions within a deep-seated reaction zone. Although temperature and pressure conditions within this region are key parameters that characterize the seafloor hydrothermal regime and the cooling of mid-ocean ridges, they are poorly constrained. In this paper, we developed a model in which high-temperature, vapor-type (low-salinity) vent fluid silica (Si) and chlorine (Cl) concentrations can be used to define lines in pressure-temperature space whose intersection is used to estimate conditions at the top of the reaction zone, under the simplifying assumption that Si and Cl reflect a common point of equilibration. We apply this model to various basaltic-hosted mid-ocean ridge sites. Results suggest a minimal variation in inferred temperatures, ranging from 415 to 445°C. This lends support to the fluxibility model in which upwelling hydrothermal plumes rise at temperatures that maximize the energy flux. Quartz precipitation due to reequilibration during upflow tends to lower temperature and pressure estimates and can artificially indicate shallower transition from reaction to upflow zone. However, maximum equilibration pressures are site-dependent and compare well with depth to magma chamber imaged by seismic studies. This suggests that vapors circulate close to magma chambers and is difficult to reconcile with models in which mid-ocean ridge hydrothermal circulation occurs in two layers with a substantial layer of convecting brine. Accordingly, equilibration pressure predicted by our model can also be used to infer the depth of the magma chamber at sites where seismic data are not available but where vapor-like fluids have been collected and analyzed.

Components: 5327 words, 5 figures, 1 table.

Keywords: hydrothermal vents; mid-ocean ridges; reaction zone; silica; chlorine; AMC depth.

Index Terms: 8135 Tectonophysics: Hydrothermal systems (0450, 1034, 3017, 3616, 4832, 8424); 3614 Mineralogy and Petrology: Mid-oceanic ridge processes (1032, 8416); 1012 Geochemistry: Reactions and phase equilibria (3612, 8412).

Received 28 January 2009; Revised 13 April 2009; Accepted 17 April 2009; Published 29 May 2009.

Fontaine, F. J., W. S. D. Wilcock, D. E. Foustoukos, and D. A. Butterfield (2009), A Si-Cl geothermobarometer for the reaction zone of high-temperature, basaltic-hosted mid-ocean ridge hydrothermal systems, *10*, Q05009, doi:10.1029/2009GC002407.

1. Introduction

[2] Hydrothermal circulation operating in young mid-ocean ridge crust (age <1 Ma) is responsible for ~10% (3–4 TW) of the global Earth heat loss [Elderfield and Schultz, 1996]. Despite such large global estimates, the impact of hydrothermal circulation on crustal temperature distribution at mid-ocean ridges are still poorly known. Classically, a single hydrothermal cell is divided into a cold recharge/downflow area, a reaction zone where the fluids heat up and react with the rock and a hot discharge/upflow zone through which the fluids rise quickly with transit time as low as about 1 h as suggested by modeling studies [e.g., Wilcock, 2004], (Figure 1). In order to be vented at black smoker–like temperatures (up to 407°C at the Turtle Pits site, 5°S on the Mid-Atlantic Ridge [German et al., 2008, Koschinski et al., 2008]), hydrothermal fluids have to be heated in the reaction zone to temperatures not much higher than 450–500°C as constrained by vent fluid chemistry [Seyfried and Ding, 1995] and predicted by numerical models of hydrothermal circulation [Wilcock, 1998; Rabinowicz et al., 1999; Jupp and Schultz, 2000; Geiger et al., 2005].

[3] The depths at which such reaction zone temperatures are reached are harder to constrain. Geophysical constraints on the depth to axial magma chambers (AMCs) only place an upper bound on the penetration depth of hydrothermal fluids (e.g., ~1.5 km at East Pacific Rise [Detrick et al., 1987], ~2.5 km at Endeavor, Juan de Fuca [Van Ark et al., 2007]). Microearthquakes are concentrated immediately above the AMC in a zone that is few hundred meters thick and are commonly interpreted in terms of thermal cracking where cold seawater removes heat from crustal rocks [Tolstoy et al., 2008; Wilcock et al., 2002]. However, the microearthquake data place only weak constraints on the temperature structure. Theoretical arguments suggest that a basal conductive boundary layer that is only about ten meters thick is required to match typical vent site heat flux of a few hundreds of MW [Lowell and Germanovich,

1994], however, the spatial relationship between this thin layer and the seismogenic zone is poorly known.

[4] The analysis of vent fluid chemistry can constrain how far above the AMC hydrothermal fluids last equilibrate. In particular, silica (Si) concentrations are often used to infer pressure conditions in hydrothermal systems under the assumption that Si concentrations in sampled fluids reflect equilibrium with quartz at high temperature [see Foustoukos and Seyfried, 2007a, and references therein]. The solubility of quartz at depth, expressed by silica geobarometer models, is thus the major control on the amount of silica in black smoker solutions [Fournier et al., 1982; Von Damm et al., 1991; Foustoukos and Seyfried, 2007a]. One drawback to the use of the silica geobarometer is that it requires knowledge of the temperature, whose a priori distribution is not well constrained in mid-ocean ridge hydrothermal systems. A second drawback is that quartz solubility is also a function of chlorinity (Cl), which will vary significantly in the high-temperature, two-phase (vapor and brine), reaction zones [Bai et al., 2003; Kawada et al., 2004; Fontaine et al., 2007].

[5] In this work we develop a simple model to infer reaction zone P-T conditions using both the Si and Cl concentrations of vent fluids, while assuming that Si and Cl equilibrate at the same time in a fluid packet leaving the reaction zone and entering the upflow zone. We show that in the two-phase area of the NaCl-H₂O system, Si and Cl form lines of isoconcentrations in the P-T space and their crossing defines a single P-T equilibration point. We apply this model to several, basaltic-hosted hydrothermal sites including the East Pacific Rise (EPR) at 9°50'N, the Main Endeavor Field on the Juan de Fuca ridge, the Lucky Strike on the Mid-Atlantic Ridge, and the South EPR at 17–19°S. For each of these sites fluid chemistry and geophysical data are published or available. Interestingly, we find a maximum depth of reaction zone that compares well with the depth to the respective AMC at each site. Thus, we suggest that our model can be used to infer the depth to heat source below

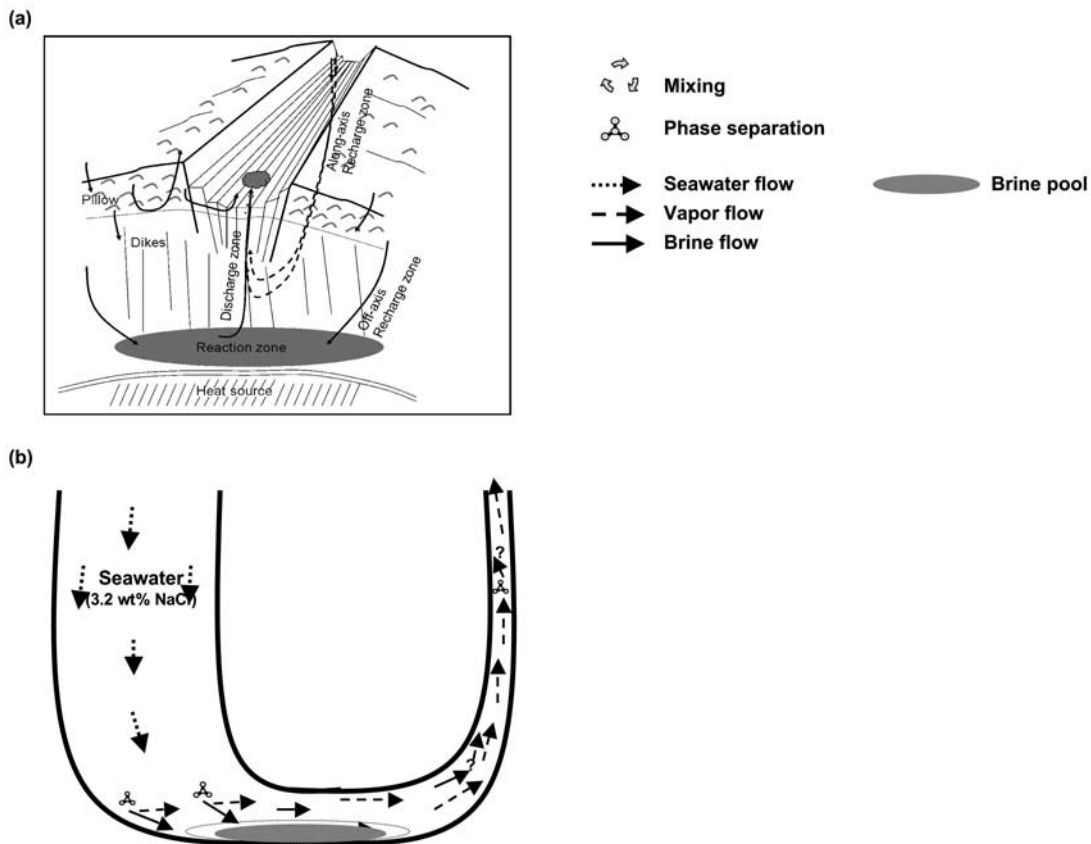


Figure 1. (a) Structure of a mid-ocean ridge hydrothermal system. Cold seawater flows in the crust in the recharge area and reaches the reaction zone at the base of the system where extensive chemical exchanges between the wall rock and seawater occur. Seawater-derived hydrothermal fluids then flow back in the upflow zone to vent at the seafloor. (b) A simplified hydrothermal cell. Cold seawater percolates in wide recharge areas and reaches the high-temperature reaction zone where it phase separates to form a vapor and a brine. Both phases flow in the reaction zone, and efficient segregation occurs within the upflow zone: low-density, low-salinity vapors rise buoyantly toward the seafloor, while brines are stored locally or rise only slowly to be stored at shallower depth [Fontaine and Wilcock, 2006]. Eventually, rising vapors can phase separate again at shallow depth. Modified after Fontaine *et al.* [2007].

fields where geophysical constraints are lacking but where black smoker-like fluids have been sampled. Our results also have important implications for the subsurface hydrology of mid-ocean ridge hydrothermal systems and internal physical characteristics of hydrothermal cells.

2. Conceptual Model

[6] Seawater-derived fluids that enter the high-temperature, supercritical ($>400^{\circ}\text{C}$) reaction zone phase separate to produce low-chlorinity (compared to seawater, $\text{Cl}_{\text{sea}} = 540 \text{ mmol/kg}$) vapors and high-chlorinity brines. Brines and vapors then segregate: low-density vapors are thought to ascend buoyantly in the system, while high-density brines are expected to accumulate at its base or rise very slowly until they reach a level of neutral

buoyancy (Figure 1b [Fontaine and Wilcock, 2006; Fontaine *et al.*, 2007]). Depending on the temperature and pressure conditions within the upflow zone, vapors can either vent directly at the seafloor with their supercritical chlorinity or undergo further phase separation (subcritical) and feed low- and high-chlorinity vents. Sampled vapors and brines vented along the global ridge network have chlorinities ranging from 5 to 250% the chlorinity of seawater, respectively [e.g., Von Damm, 1995]. Although subcritical phase separation has been observed at some sites [e.g., Butterfield *et al.*, 1990], in most vapor-dominated systems vented vapors are thought to acquire their chlorinity at supercritical conditions near the base of the system [e.g., Butterfield *et al.*, 1994; Foustoukos and Seyfried, 2007a; Fontaine and Wilcock, 2006] and then rise quickly to the seafloor [e.g., Wilcock, 2004]. The silica concentration of these vapors in

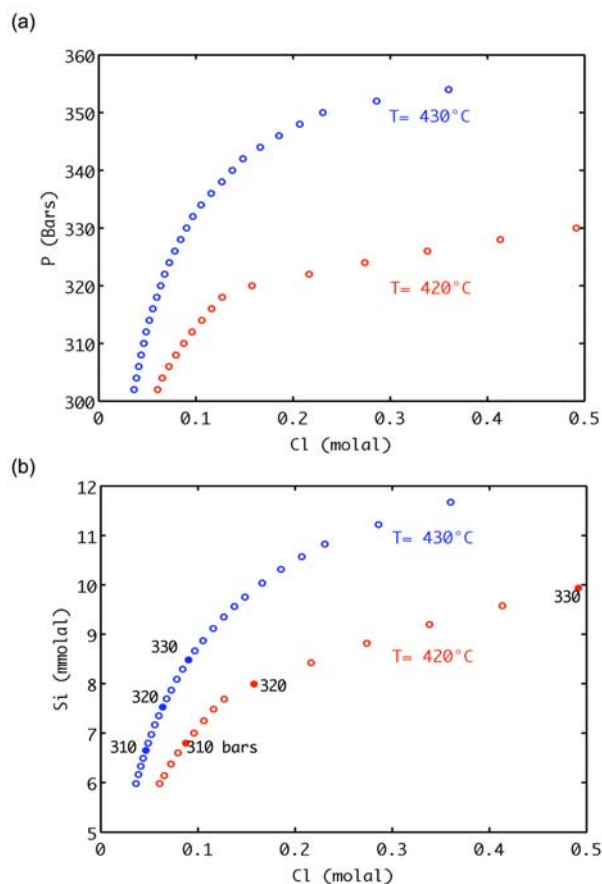


Figure 2. (a) Chlorinity of vapor-like fluids in the two-phase area as a function of pressure for two temperatures. Calculations were made using the thermodynamical relationships of Berndt et al. (presented paper, 2001). (b) Silica concentrations as a function of chlorinity along the two vapor branches shown in Figure 2a. Calculations were made using the quartz solubility equation of *Foustoukos and Seyfried* [2007a].

equilibrium with quartz is thus likely to reflect conditions that approximate the boundary between the reaction and upflow zones.

[7] In the two-phase reaction zone at the base of the system, vapor salinities are a function of temperature and pressure only (M. E. Berndt et al., Phase separation and two-phase flow in seafloor hydrothermal systems: Geophysical modeling in the NaCl-H₂O system, paper presented at the Eleventh Annual V. M. Goldschmidt Conference, Geochemical Society, Hot Springs, Virginia, 2001) (Figure 2a). Silica concentrations that are function of temperature, pressure and chlorinity can then be calculated along the vapor branch using the relationship derived by *Foustoukos and Seyfried* [2007a] (Figure 2b). Using curves such as those shown in Figures 2a and 2b, we plot on Figure 3,

silica (from 5 to 17 mmolal) and chlorine (from 0.05 to 0.5 molal) “isoconcentration” lines in a pressure-temperature space that corresponds to conditions within the NaCl-H₂O two-phase region. The quadratic regression equation given by *Foustoukos and Seyfried* [2007a] for quartz solubility gives satisfactory Si isolines for values up to Si = 14 mmolal. For Si concentrations greater than 14 mmolal, this equation does not hold anymore as the pressure and temperature ranges are too far from the experimental P-T conditions (235–381 bars and 390–430°C). Accordingly, for Si > 14 mmolal we simply linearly extrapolate the isolines. Intersections between lines of isosilica and isochlorine define a single pressure-temperature equilibration point that can be used to infer conditions at the boundary between the reaction and upflow zones.

3. Discussion and Interpretation

[8] The equilibration point of several vapor-like, black smoker vents of the EPR at 9°50'N, Main Endeavor Field, Lucky Strike Field and EPR at 17–19°S (see data in Table 1) are plotted in Figure 3. Here, dissolved Cl and Si concentrations measured in vent fluids are plotted along the isoconcentration lines, constraining in this way the pressure and temperature conditions of quartz-fluid equilibrium. Some of these vents (e.g., at EPR 9°50'N and Main Endeavor Field) have been venting low-salinity vapors over at least a decade [*Von Damm*, 2004; *Butterfield et al.*, 1994; *Lilley et al.*, 2003], while very little is known about the pressure/temperature conditions that dictate mineral-fluid interactions deep in the reaction zone. All the equilibration points plot at supercritical pressure and temperature, with respect to 3.2 wt % NaCl-seawater (critical points at 300 bars, 410°C). This clearly illustrates the establishment of supercritical conditions for the low-salinity vapor fluids at the EPR and Main Endeavor Field, being in accordance with previous estimations [*Foustoukos and Seyfried*, 2007a; *Foustoukos and Seyfried*, 2007b; *Seyfried et al.*, 2003].

[9] Furthermore, when applied to vapor-like fluids of the EPR at 9°50'N, Main Endeavor Field, Lucky Strike field and EPR at 17–19°S, this Si-Cl geothermobarometer predicts maximum reaction zone pressures that compare well with the depth to the AMCs. Assuming that hydrothermal cells operate in a pressure gradient of ~800 kg/m³ which is fairly close to cold hydrostatic as predicted by models [e.g., *Jupp and Schultz*, 2004; *Fontaine*

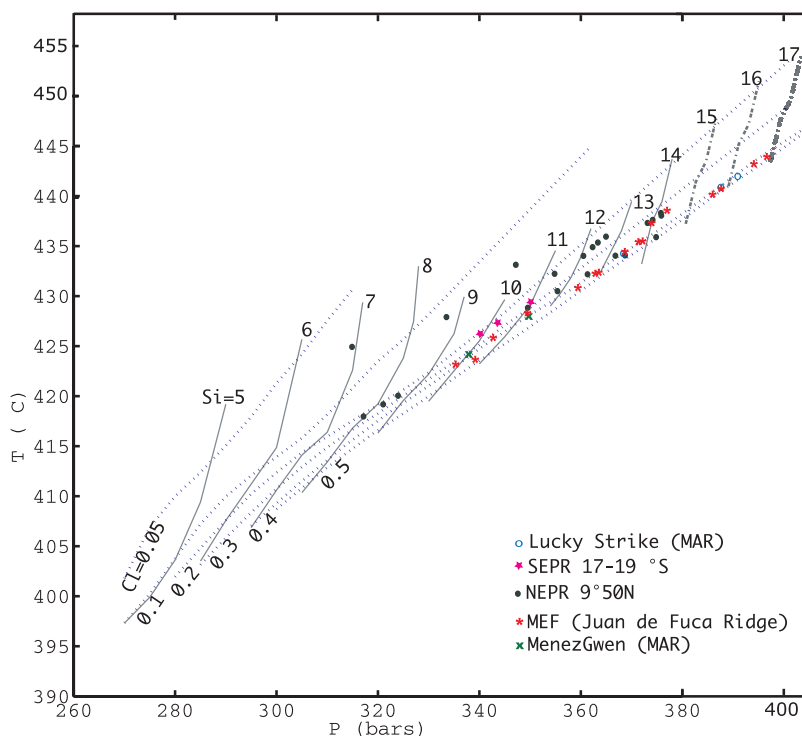


Figure 3. Chlorinity (in molal, dotted lines) and silica (in mmolal, bold solid and dot-dashed lines) isoconcentration lines in P-T space. For silica, solid lines indicate curves constrained directly by experimental data while dot-dashed lines are based on an extrapolation. Intersection of iso-Cl and iso-Si defines a single P-T equilibration point. Estimated equilibration points for high-temperature, vapor-like vents of the Main Endeavor Field (MEF), EPR-9°50'N, EPR 17–19°S, Lucky Strike (MAR), and Menez Gwen (MAR) vent fields suggest conditions of mineral-fluid equilibria at temperatures higher than 415°C, clearly indicating the dominant role of supercritical phase separation in deep-crustal hydrothermal circulation.

and Wilcock, 2006] we have calculated the depths to the transition between the reaction and upflow zones using maximum equilibration pressures for each fields. We find that these depths are in good agreement with the depth to the AMC for the sites where seismic data are available (Figure 4). At the 9°50'N and 17–19°S areas on the EPR particularly, the depth to the transition between reaction and upflow zones up to 1500 m and 1000 m bsf, respectively, suggests vapor circulation very close to the AMC in agreement with recent numerical simulations of hydrothermal two-phase flow by Coumou *et al.* [2009] producing large vapor-dominated regions close to the magma chamber, with the brine being trapped away from the magmatic heat source. This supports the inference from modeling studies that hydrothermal systems are separated from the magma chamber by a thin conductive boundary layer [Lister, 1974; Lowell and Germanovich, 1994]. It also lends support to recent models inferring slow upward brine movement and shallow storage below vapor-dominated hydrothermal vent sites [Fontaine and Wilcock, 2006; Coumou *et al.*, 2009] rather than sequestra-

tion within a deep, hundreds of meters thick basal layer [Bischoff and Rosenbauer, 1989]. Finally it also suggests that the Si-Cl geothermobarometer can be used to infer the depth to the heat source/magma chambers at black smoker sites where geophysical experiments (e.g., seismic, magnetic) are lacking but where vapor-rich hydrothermal fluids have been sampled. At the Menez Gwen site for example, maximum equilibration pressures suggest a heat source at a depth of 3000–3400 m bsf (Figure 4).

[10] It is important to note that while the maximum pressures match the magma chamber depth, many of the individual equilibration points indicate significantly shallower depths, down to 700 m bsf at the EPR and 1500 m at the MEF, for example. One possible explanation is quartz precipitation during upflow as suggested by kinetic models of water-rock interaction applied to problems of silica mass transfer [Wells and Ghiorso, 1991]. Such re-equilibration processes would lower vent fluid silica concentrations and lead to underestimates of the depth of equilibration and transition from reaction

Table 1. Selected Cl and Si Concentrations for High-Temperature Hydrothermal Fluids^a

Location	Si (mmol)	Cl (mmol)
<i>EPR-9°N</i>		
B9' vent ^b		
1	12.4	249
2	14	330
6	13.4	473
8	11.7	349
10	7.98	217
B9cplx vent ^b	12.5	390
B9'' vent ^b		
1	8.55	243
B9 ^b		
1	9.9	154
2	6.98	75,5
3	11.3	212
4	12.1	263
5	12.6	267
6	13.9	325
7	14.1	330
9	13.2	400
10	12.8	401
12	11	306
13	8.15	226
P vent ^b		
1	8.7	135
5	12.3	262
6	14.2	347
18	14.2	500
MEF		
Sully vent ^c	12.5	434,1
	13.8	459,7
	9.8	352,6
	13	461,3
	11.1	374,4
	13.4	436,1
	10.6	348,6
S&M vent ^c	14	370
	14.4	356
	15.4	470
	17	477
Hulk vent ^c		
Hulk vent ^d		
M3468D	12.9	433
M3468C	13.7	423
Grotto vent ^c	15.7	425
Crypto vent ^c	16.6	479
Dante vent ^d		
M3470B	10.7	457
<i>SEPR^c</i>		
03-G	9.95	212
08-G	11	283
09-D	10.2	251
<i>Menez Gwen^f</i>		
MGw 1994	10	374
MGw 1997	11.2	398
<i>Lucky Strike^f</i>		
EiffelTower 1994	13.3	417
MrkUS4 1997	15.7	431
MrkUS4 1993	16.1	440

to upflow zone. An alternative is that part of the upflow zone is in the two-phase area with vapors and brines segregating at shallower depth (P-T path 2 on Figure 5), as it has been suggested for some vents at the Main Endeavor Field [Butterfield *et al.*, 1994] and observed in numerical simulations of two-phase flow in the NaCl-H₂O system [Coumou *et al.*, 2009]. In this last scenario, the estimated temperature gradient at the base of the system would vary between samples and Si-Cl inferred P-T would not always correspond to the reaction–upflow zone interface. Samples with shallower calculated equilibration depths (P-T path 2 in Figure 5) likely reflect conditions of lower-temperature gradients at the transition between the reaction and upflow zones compared to the ones with larger depths (P-T path 1 in Figure 5), which can also reconcile with supercritical phase separation and segregation phenomena along the discharge pathway.

[11] Another intriguing finding of our analysis is the narrow range of equilibration temperatures from 415°C to 445°C. Rock geochemical data suggest fluid percolation at temperature up to at least 750°C [e.g., Gillis *et al.*, 2001; Manning *et al.*, 1996], but equilibration points indicate reaction zone temperatures are ~300°C lower. This is most likely because the Si-Cl geothermobarometer reflects only the last point of reequilibration at the top of the reaction zone. This narrow range of temperatures also lends support to the fluxibility (a measure of the ability of buoyancy-driven water to transport energy) argument stating that hydrothermal plumes arise where the advective heat flux is optimized [Jupp and Schultz, 2000; Geiger *et al.*, 2005]. Initial thermodynamical calculations based on pure water properties [Jupp and Schultz, 2000] indicate that fluxibility is maximized at temperature ~400°C, but for salt-bearing, vapor-like fluids this value would be shifted to a few tens of degree Celsius higher [Geiger *et al.*, 2005] in agreement with our reaction zone temperatures.

[12] Here we apply the method of finding the intersection of silica solubility and chloride composition to vapor phases in equilibrium with corresponding brines, to find a unique solution in

Notes to Table 1:

^a Fluids collected at EPR 9°50 N, Main Endeavour Field (Juan de Fuca Ridge), EPR 17–19°S, Lucky Strike (MAR), and Menez Gwen (MAR).

^b Von Damm [2004].

^c This study.

^d Seyfried *et al.* [2003].

^e Charlou *et al.* [1996].

^f Charlou *et al.* [2000].

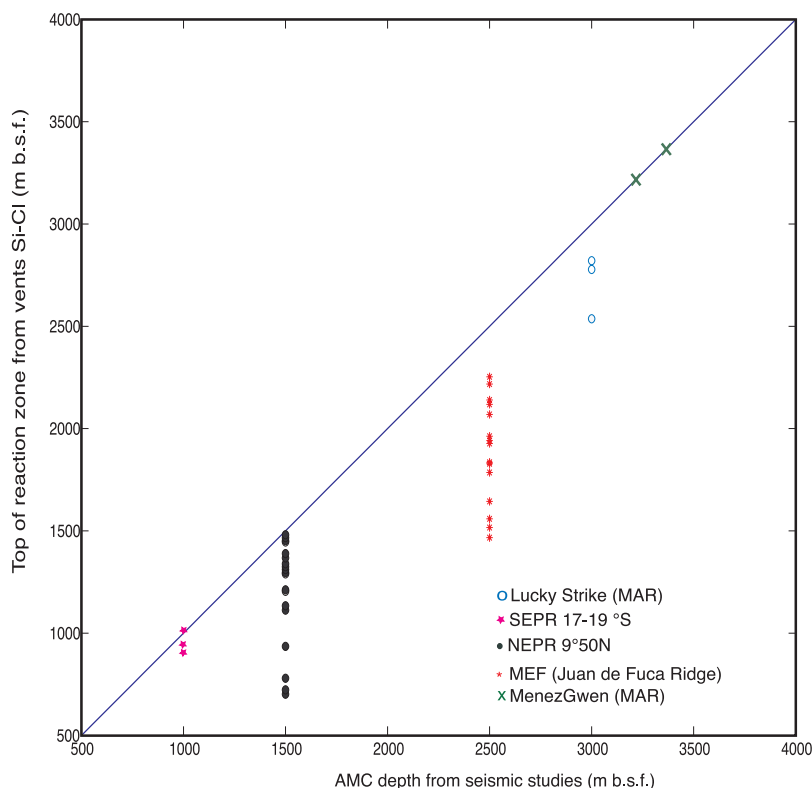


Figure 4. Si-Cl-inferred depth to the top of the reaction zone versus depth to AMC inferred from seismic studies for the five hydrothermal sites of Figure 3. Calculations were made assuming hydrothermal cells operate in a cold hydrostatic pressure gradients where $\rho_{\text{cold}} = 800 \text{ kg/m}^3$. If $\rho_{\text{cold}} = 900 \text{ kg/m}^3$, the Si-Cl-inferred depth would be reduced by $\sim 10\%$. For the Menez Gwen site where the depth to the AMC/heat source is not known, Si-Cl-inferred depth to the top of the reaction are plotted as green crosses on the $x = y$ axis.

temperature-pressure space. The same general approach could be applied to brines, if brines were to vent directly from the reaction zone to the seafloor. However, the densities of many brines are high enough that they do not vent [e.g., Fontaine and Wilcock, 2006], and for those that do their history of mixing may be more complicated because they will rise more slowly. Moreover, there are no experimental data on silica-brine equilibria under phase separation conditions.

[13] Finally, the underlying assumptions that must be considered when applying our Si-Cl geothermobarometer are that a pure vapor phase in equilibrium with quartz along the two-phase curve exits the reaction zone and reaches the seafloor without changing the Si and Cl composition. Incomplete segregation of brine and vapor from a two-phase vapor-liquid zone would raise the Si and Cl content and shift the inferred vapor equilibrium conditions to higher pressure and temperature. Mixing between cold seawater into a vapor at depth followed by Mg precipitation would lower Si content and raise Cl, and these variations have opposite

effects on the equilibrium temperatures and pressures (Figure 3). However, the amount of mixing will depend critically on the vapor velocities and estimated residence time lower than 1 h during upflow [e.g., Wilcock, 2004] may tend to minimize mixing processes. Real systems will depart from the ideal case, and these caveats have to be considered when applying our model. If one interprets variation in Cl and Si within a single vent field to be the result of variable mixing between a vapor and a brine, then only fluids with the lowest Cl should be subject to the intersecting isoline treatment. Alternatively, variation in Cl and Si within a field could be interpreted in terms of multiple zones of phase separation. In that case, the intersecting isoline treatment would yield the range in reaction zone temperatures and pressures.

[14] Despite these caveats, we note that the model does not overpredict the depths to the top of the reaction zone based on independent estimates of depth of AMCs. Furthermore, the predicted reaction zone temperatures are consistent with the fluxibility argument. Thus, we suggest that the

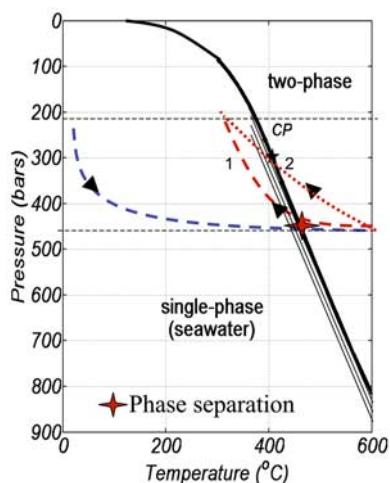


Figure 5. Possible interpretations of equilibration points in Figure 3. Set of two-phase curves for seawater (thick line) and lower-salinity fluids (thinner lines). In blue and red are possible thermodynamical paths for hydrothermal fluids in the recharge and discharge zones, respectively. Path 1 (dashed line) is seawater that downwells in recharge zone and phase separates at the base of the system. Most of the upflow zone is in the single-phase area because of high-temperature gradients at the base of the system [Fontaine *et al.*, 2007]. Vented low-chlorinity vapor compositions reflect temperature and pressure of a deeply seated reaction zone. Path 2 (dotted line) is the same as path 1, but part of the upflow is in the two-phase area because of lower-temperature gradients at the base of the upflow zone. Vented low-chlorinity vapors reflect shallower T-P conditions. Nevertheless, for each path, kinetically driven quartz precipitation during upflow could lower vent fluid silica concentrations and lead to an underestimate of the equilibration pressure and thus of the depth of the transition between reaction and upflow zones.

departures of our idealized model from real systems are sufficiently small that it provides a useful method to predict the depth and temperature of reaction zones in mid-ocean ridge hydrothermal systems and by inference the depth of the heat source immediately underneath.

4. Conclusion

[15] In this work we show that the Cl and Si concentrations of vapor-like fluids vented at black smoker fields along the mid-ocean ridge network can be used to infer reaction zone depths. The maximum predicted depths at several sites are in good agreement with seismic measurement of the depth of the AMC and so we infer that the method provides a means to estimate the depth of an AMC when no seismic images are available. Detailed

analysis of equilibration points derived from the Si-Cl geothermobarometer may also help constrain the physical state of upflow zones and the vertical extent of two-phase flow within the crust. Si-Cl-derived reaction zone temperatures are also consistent with theoretical models of the dynamics of submarine high-temperature hydrothermal systems which predict that convective cells are organized to optimize upward heat flux and upflow zones occurs at temperatures around 420–450°C [Jupp and Schultz, 2000; Geiger *et al.*, 2005].

Acknowledgments

[16] We thank Dim Coumou, Mike Mottl, and the Associate Editor William Seyfried for their thorough reviews that improved earlier versions of this manuscript and Javier Escartin for helpful discussions. Publication of this work was supported by the National Science Foundation, grant OCE-0243395, and by the Agence National de la Recherche, grant “MOTHSEIM” NT05-3-42213. This is Institut de Physique du Globe de Paris contribution 2499.

References

- Bai, W., W. Xu, and R. P. Lowell (2003), The dynamics of submarine geothermal heat pipes, *Geophys. Res. Lett.*, *30*(3), 1108, doi:10.1029/2002GL016176.
- Bischoff, J. L., and R. J. Rosenbauer (1989), Salinity variations in submarine hydrothermal systems by layered double-diffusive convection, *J. Geol.*, *97*, 613–623.
- Butterfield, D. A., G. J. Massoth, R. E. McDuff, J. E. Lupton, and M. D. Lilley (1990), Geochemistry of hydrothermal fluids from axial seamount hydrothermal emissions study vent field, Juan de Fuca Ridge: Subseafloor boiling and subsequent fluid-rock interaction, *J. Geophys. Res.*, *95*(B8), 12,895–12,921, doi:10.1029/JB095iB08p12895.
- Butterfield, D. A., R. E. McDuff, M. J. Mottl, M. D. Lilley, J. E. Lupton, and G. J. Massoth (1994), Gradients in the composition of hydrothermal fluids from the Endeavour segment vent field: Phase separation and brine loss, *J. Geophys. Res.*, *99*, 9561–9583, doi:10.1029/93JB03132.
- Charlou, J. L., Y. Fouquet, J. P. Donval, J. M. Auzende, P. Jean-Baptiste, M. Stievenard, and S. Michel (1996), Mineral and gas chemistry of hydrothermal fluids on an ultrafast spreading ridge: East Pacific Rise, 17° to 19°S (Naudur cruise, 1993) phase separation processes controlled by volcanic and tectonic activity, *J. Geophys. Res.*, *101*, 15,899–15,919, doi:10.1029/96JB00880.
- Charlou, J. L., J. P. Donval, E. Douville, P. Jean-Baptiste, J. Radford-Knoery, Y. Fouquet, A. Dapigny, and M. Stievenard (2000), Compared geochemical signatures and the evolution of Menez Gwen (37°50'N) and Lucky Strike (37°17'N) hydrothermal fluids, south of the Azores Triple Junction on the Mid-Atlantic Ridge, *Chem. Geol.*, *171*, 49–75, doi:10.1016/S0009-2541(00)00244-8.
- Coumou, D., T. Driesner, P. Weis, and C. A. Heinrich (2009), Phase separation, brine formation, and salinity variation at Black Smoker hydrothermal systems, *J. Geophys. Res.*, *114*, B03212, doi:10.1029/2008JB005764.
- Detrick, R. S., P. Buhl, E. Vera, J. Mutter, J. Orcutt, J. Madsen, and T. Brocher (1987), Multichannel seismic imaging of a

- crustal magma chamber along the East Pacific Rise between 9°N and 13°N, *Nature*, *326*, 35–41, doi:10.1038/326035a0.
- Elderfield, H., and A. Schultz (1996), Mid-ocean ridge hydrothermal fluxes and the chemical composition of the ocean, *Annu. Rev. Earth Planet. Sci.*, *24*, 191–224, doi:10.1146/annurev.earth.24.1.191.
- Fontaine, F. J., and W. S. D. Wilcock (2006), The dynamics and storage of brines in mid-ocean ridges hydrothermal systems *J. Geophys. Res.*, *111*, B06102, doi:10.1029/2005JB003866.
- Fontaine, F. J., W. S. D. Wilcock, and D. A. Butterfield (2007), Physical controls on the salinity of mid-ocean ridge hydrothermal vent fluids, *Earth Planet. Sci. Lett.*, *257*, 132–145, doi:10.1016/j.epsl.2007.02.027.
- Fournier, R. O., R. J. Rosenbauer, and J. L. Bischoff (1982), The solubility of quartz in aqueous sodium chloride solution at 350°C and 180 to 500 bars, *Geochim. Cosmochim. Acta*, *46*, 1975–1978, doi:10.1016/0016-7037(82)90136-3.
- Foustoukos, D. I., and W. E. Seyfried Jr. (2007a), Quartz solubility in the two-phase and critical region of the NaCl–KCl–H₂O system: Implications for submarine hydrothermal vent systems at 9°50′N East Pacific Rise, *Geochim. Cosmochim. Acta*, *71*, 186–201, doi:10.1016/j.gca.2006.08.038.
- Foustoukos, D. I., and W. E. Seyfried, Jr. (2007b), Trace element partitioning between vapor, brine and halite under extreme phase separation conditions, *Geochim. Cosmochim. Acta*, *71*, 2056–2071, doi:10.1016/j.gca.2007.01.024.
- Geiger, S., T. Driesner, C. A. Heinrich, and S. K. Matthäi (2005), On the dynamics of NaCl–H₂O fluid convection in the Earth's crust, *J. Geophys. Res.*, *110*, B07101, doi:10.1029/2004JB003362.
- German, C. R., et al. (2008), Hydrothermal activity on the southern Mid-Atlantic Ridge: Tectonically and volcanically controlled venting at 4–5°S, *Earth Planet. Sci. Lett.*, *273*, 332–344, doi:10.1016/j.epsl.2008.06.048.
- Gillis, K. M., K. Muehlenbachs, M. Stewart, T. Gleeson, and J. Karson (2001), Fluid flow patterns in fast spreading East Pacific Rise crust exposed at Hess Deep, *J. Geophys. Res.*, *106*, 26,311–26,330, doi:10.1029/2000JB000038.
- Jupp, T., and A. Schultz (2000), A thermodynamic explanation for black smoker temperatures, *Nature*, *403*, 880–883, doi:10.1038/35002552.
- Jupp, T., and A. Schultz (2004), Physical balances in subseafloor hydrothermal convection cells, *J. Geophys. Res.*, *109*, B05101, doi:10.1029/2003JB002697.
- Kawada, Y., S. Yoshida, and S. Watanabe (2004), Numerical simulations of mid-ocean ridge hydrothermal circulation including the phase separation of seawater, *Earth Planets Space*, *56*, 193–215.
- Koschinsky, A., D. Garbe-Schönberg, S. Sander, K. Schmidt, H.-H. Gennerich, and H. Strauss (2008), Hydrothermal venting at pressure-temperature conditions above the critical point of seawater, 5°S on the Mid-Atlantic Ridge, *Geology*, *36*, 615–618, doi:10.1130/G24726A.1.
- Lilley, M. D., D. A. Butterfield, J. E. Lupton, and E. J. Olson (2003), Magmatic events can produce rapid changes in hydrothermal vent chemistry, *Nature*, *422*, 878–881, doi:10.1038/nature01569.
- Lister, C. R. D. (1974), On the penetration of water into hot rock, *Geophys. J. R. Astron. Soc.*, *39*, 465–509.
- Lowell, R. P., and L. N. Germanovich (1994), On the temporal evolution of high-temperature hydrothermal systems at ocean ridge crests, *J. Geophys. Res.*, *99*, 565–575, doi:10.1029/93JB02568.
- Manning, C. E., P. E. Weston, and K. I. Mahon (1996), Rapid high-temperature metamorphism of East Pacific Rise gabbros from Hess Deep, *Earth Planet. Sci. Lett.*, *144*, 123–132, doi:10.1016/0012-821X(96)00153-7.
- Rabinowicz, M., J.-C. Sempère, and P. Genthon (1999), Thermal convection in a vertical permeable slot: Implications for hydrothermal circulation along mid-ocean ridges, *J. Geophys. Res.*, *104*, 29,275–29,292, doi:10.1029/1999JB900259.
- Seyfried, W. E., Jr., and K. Ding (1995), Phase equilibria in subseafloor hydrothermal systems: A review of the role of redox, temperature, pH and dissolved Cl on the chemistry of hot spring fluids at mid-ocean ridges, in *Seafloor Hydrothermal Systems: Physical, Chemical, Biological and Geological Interactions*, *Geophys. Monogr. Ser.*, vol. 91, edited by S. E. Humphris et al., pp. 249–272, AGU, Washington, D. C.
- Seyfried, W. E., Jr., J. S. Seewald, M. E. Berndt, K. Ding, and D. I. Foustoukos (2003), Chemistry of hydrothermal vent fluids from the Main Endeavour Field, northern Juan de Fuca Ridge: Geochemical controls in the aftermath of June 1999 seismic events, *J. Geophys. Res.*, *108*(B9), 2429, doi:10.1029/2002JB001957.
- Tolstoy, M., F. Waldhauser, D. R. Bohnenstiehl, R. T. Weekley, and W.-Y. Kim (2008), Seismic identification of along-axis hydrothermal flow on the East Pacific Rise, *Nature*, *451*, 181–184, doi:10.1038/nature06424.
- Van Ark, E. M., R. S. Detrick, J. P. Canales, S. M. Carbotte, A. J. Harding, G. M. Kent, M. R. Nedimovic, W. S. D. Wilcock, J. B. Diebold, and J. M. Babcock (2007), Seismic structure of the Endeavour Segment, Juan de Fuca Ridge: Correlations with seismicity and hydrothermal activity, *J. Geophys. Res.*, *112*, B02401, doi:10.1029/2005JB004210.
- Von Damm, K. L. (1995), Control on the chemistry and temporal variability of seafloor hydrothermal fluids, in *Seafloor Hydrothermal Systems: Physical, Chemical, Biological and Geological Interactions*, *Geophys. Monogr. Ser.*, vol. 91, edited by S. E. Humphris et al., pp. 222–247, AGU, Washington, D. C.
- Von Damm, K. L. (2004), Evolution of the hydrothermal system at East Pacific Rise 9°50′N: Geochemical evidence for changes in the upper oceanic crust, in *Mid-Ocean Ridges: Hydrothermal Interactions Between the Lithosphere and Oceans*, *Geophys. Monogr. Ser.*, vol. 148, edited by C. R. German et al., pp. 285–304, AGU, Washington, D. C.
- Von Damm, K. L., J. L. Bischoff, and R. J. Rosenbauer (1991), Quartz solubility in hydrothermal seawater: An experimental study and equation describing quartz solubility for up to 0.5 M NaCl solutions, *Am. J. Sci.*, *291*, 977–1007.
- Wells, J. T., and M. S. Ghiorso (1991), Coupled fluid flow and reaction in mid-ocean ridge hydrothermal systems: The behavior of silica, *Geochim. Cosmochim. Acta*, *55*, 2467–2481, doi:10.1016/0016-7037(91)90366-D.
- Wilcock, W. S. D. (1998), Cellular convection models of mid-ocean ridge hydrothermal circulation and the temperatures of black smoker fluids, *J. Geophys. Res.*, *103*, 2585–2596, doi:10.1029/97JB03252.
- Wilcock, W. S. D. (2004), The physical response of mid-ocean ridge hydrothermal systems to local earthquakes, *Geochim. Geophys. Geosyst.*, *5*, Q11009, doi:10.1029/2004GC000701.
- Wilcock, W. S. D., S. A. Archer, and G. M. Purdy (2002), Microearthquakes on the Endeavour segment of the Juan de Fuca Ridge, *J. Geophys. Res.*, *107*(B12), 2336, doi:10.1029/2001JB000505.